

## Validity of the Coulomb-Born approximation for ( $e,2e$ ) reactions

D. H. Jakubassa-Amundsen

*Physics Section, University of Munich, 85748 Garching, Germany*

(Received 4 August 1995; revised manuscript received 31 October 1995)

The Coulomb-Born approximation (CBA) is tested against experiment and against the distorted-wave Born approximation (DWBA) for target inner-shell ionization by fast electrons. It is found that the CBA is fairly accurate in the binary region for the heavy systems when relativistic effects play a minor role. However, CBA underestimates the cross sections in the recoil region for the heavy targets, but also in the binary region for light targets. This is caused by an inappropriate representation of the electronic wave functions, and is neither a deficiency of a first-order theory nor due to lack of orthogonality in the present form of the CBA.

PACS number(s): 34.80.Dp

### I. INTRODUCTION

With the advent of the relativistic distorted-wave Born approximation (DWBA) [1] the momentum distribution of the two outgoing electrons in fast ( $e,2e$ ) collisions can in most cases be well described for any target ranging from helium [2] to uranium [3]. This relativistic theory, as well as the conventional DWBA [4], is applicable as long as the collision parameters allow for a first-order treatment of the interaction between the impinging and the ejected electron. The great merit of the DWBA is the accurate inclusion of the central atomic field in the construction of all bound and unbound states of the two active electrons.

The DWBA thus takes care of three important effects: (a) screening of the target nuclear field by the passive electrons; (b) relativistic contraction of the electronic wave functions in coordinate space; (c) mutual orthogonality between bound and continuum states to the extent that the identical potential is used for constructing all electronic eigenstates.

To understand the underlying physics it is instructive to study the above effects separately. Violation of orthogonality has been investigated for both nonrelativistic [5] and relativistic [6] collision systems in the framework of the plane-wave Born approximation (PWBA) where all continuum electrons are in field-free states, and dramatic effects have been found. The PWBA provides, however, in general a rather poor description of ( $e,2e$ ) reactions [6,7], pointing to the importance of including the electron-target interaction nonperturbatively. Screening effects were estimated within the plane-wave DWBA (where only the ejected electron is in a true target eigenstate, while the projectile electron moves field free) by comparing results obtained with numerically generated target eigenstates on one hand and with Coulomb functions on the other hand [24]. Also, Coulomb waves with different effective charges were compared [7], and large effects were found. However, also the plane-wave DWBA fails to describe experiment [9,10], particularly for heavy targets [8,11]. An investigation of the effects (a)–(c) within the PWBA or the plane-wave DWBA is therefore not very promising because these effects will be obscured by the incomplete inclusion of the electron-target interaction.

The present work is aimed at isolating the effects (a)–(c) with the help of the Coulomb-Born approximation (CBA) [12,13]. The CBA includes the electron-target interaction

nonperturbatively and hence is of DWBA type, but the target field is approximated by an effective Coulomb potential. Moreover, in the relativistic case, the exact Coulomb functions are substituted by a Darwin function for the bound state and by product functions (a nonrelativistic Coulomb wave times a free Dirac spinor) for all continuum states [12]. This implies that the deviations between CBA and DWBA are exclusively due to the effects of interest, screening, relativistic effects, and nonorthogonality. By comparing with an orthogonalized version of the CBA we will show that orthogonality indeed plays a minor role, since it is conserved for nonrelativistic systems and only violated in the relativistic case.

Within the CBA, screening effects are readily isolated by selecting light collision systems for the comparison between

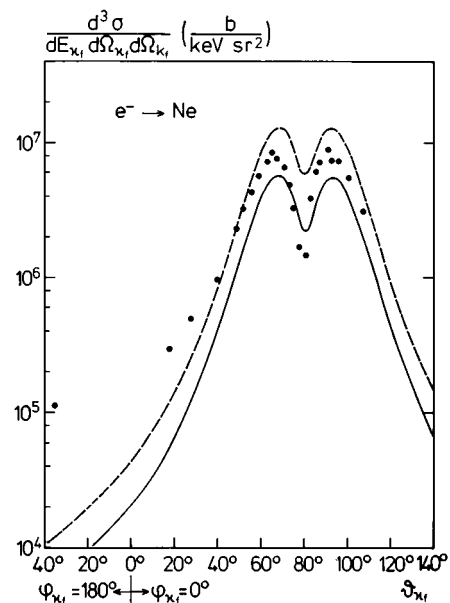


FIG. 1. Triply differential cross section for  $2p$  subshell ( $L_2 + L_3$ ) ionization of Ne by 8.2216-keV electrons in coplanar geometry as a function of ejection angle  $\vartheta_{k_f}$ . The kinetic energies of the scattered and the ejected electron are 8 and 0.2 keV, respectively, the scattering angle is  $\vartheta_{k_f} = 9.44^\circ$ , and the azimuthal angle is taken as  $\varphi_{k_f} = 180^\circ$ . Experiment: ● Daoud *et al.* [7]. Theory: —, CBA with  $Z_{\text{eff}} = 4.24$ ; - - - -, PWBA with  $Z_{\text{eff}} = 4.24$ .

CBA and DWBA or experiment, where relativistic effects are absent. On the other hand, an exclusive study of relativistic effects is possible through the investigation of electron ejection from the innermost shells of very heavy targets where screening can be neglected. We will present results for  $K$ -shell ionization of silver and gold at impact energies of 300–500 keV, and for  $L$ -subshell ionization of Ne and Ar at 3–8 keV, and of Ag at 500 keV. Section II gives a short outline of the CBA theory, which is applied in Sec. III to light targets. Section IV is devoted to heavy targets where also predictions are made concerning structures in the electron spectra from  $L_3$ -subshell ionization and the angular distribution of the electrons for noncoplanar geometry. Nonorthogonality is discussed in Sec. V and the conclusion is drawn in Sec. VI. Atomic units ( $\hbar = m = e = 1$ ) are used unless otherwise indicated.

## II. OUTLINE OF THE CBA THEORY

The Coulomb-Born approximation is a first-order theory with respect to the mutual interaction of the projectile electron and the active target electron. This means that final-state interactions of the two electrons are excluded such that the theory should only be used for energetic collisions provided the outgoing electrons are not too close in momentum space. The CBA is described in detail in previous work [12]. Briefly, the transition matrix element for electron impact ionization from an initial state  $\phi_i^{(\sigma_i)}$  with energy  $E_i$  to a final state  $\phi_f^{(\sigma_f)}$  while the projectile electron is scattered from the state  $\psi_i^{(s_i)}$  into the final state  $\psi_f^{(s_f)}$  is proportional to

$$W_{s_f \sigma_f s_i \sigma_i}^d(\mathbf{k}_f, \boldsymbol{\kappa}_f) = \int \frac{d\mathbf{q}}{q^2 - q_0^2 - i\epsilon} \langle \psi_f^{(s_f)}(\mathbf{r}_1) \phi_f^{(\sigma_f)}(\mathbf{r}_2) | e^{i\mathbf{q} \cdot (\mathbf{r}_2 - \mathbf{r}_1)} (1 - \boldsymbol{\alpha}_1 \boldsymbol{\alpha}_2) | \psi_i^{(s_i)}(\mathbf{r}_1) \phi_i^{(\sigma_i)}(\mathbf{r}_2) \rangle, \quad (2.1)$$

where  $\sigma_i$ ,  $\sigma_f$ ,  $s_i$ , and  $s_f$  are the spin quantum numbers of the electronic states. The transition is mediated by the relativistic Fourier-transformed electromagnetic interaction [14,15] with  $\boldsymbol{\alpha}_1, \boldsymbol{\alpha}_2$  Dirac matrices for the two electrons, and  $q_0 = (E_{k_i} - E_{k_f})/c$ . The momenta of projectile and active target electron are denoted by  $\mathbf{k}_i$ ,  $\mathbf{k}_f$ , and  $\boldsymbol{\kappa}_f$ , respectively, and the energy of the unbound states is related to the momentum in the usual way,  $E_k = (m^2 c^4 + k^2 c^2)^{1/2}$ . In the nonrelativistic case, all four electronic states are eigenstates to the same model potential,  $V(r) = -Z_{\text{eff}}/r$  (with  $r = r_1, r_2$ ). For relativistic collision systems, the bound state  $\phi_i^{(\sigma_i)}$  is approximated by a semirelativistic Darwin function [14], whereas the continuum states are represented by the nonrelativistic Coulomb waves times a free Dirac spinor. Although the Darwin functions correctly reproduce the relativistic angular dependence, their radial parts are only correct to first order in  $Z_{\text{eff}}\alpha = Z_{\text{eff}}/c$  and hence disregard the relativistic spatial contraction ( $r^{\gamma-1}$ ).

From (2.1), the triply differential cross section for ejecting one electron into the solid angle  $d\Omega_{k_f}$  and the other into  $d\Omega_{\kappa_f}$  is readily calculated:

$$\frac{d^3\sigma}{dE_{\kappa_f} d\Omega_{\kappa_f} d\Omega_{k_f}} = \frac{N_i}{c^6 k_i^2} \kappa_f E_{\kappa_f} k_f E_{k_f} E_{k_i} \sum_{s_f \sigma_f s_i \sigma_i} |W_{s_f \sigma_f s_i \sigma_i}^d(\mathbf{k}_f, \boldsymbol{\kappa}_f) - W_{s_f \sigma_f s_i \sigma_i}^{(\text{ex})}(\mathbf{k}_f, \boldsymbol{\kappa}_f)|^2, \quad (2.2)$$

where energy conservation implies

$$E_{k_i} + E_i = E_{k_f} + E_{\kappa_f} \quad (2.3)$$

and the exchange term  $W_{s_f \sigma_f s_i \sigma_i}^{(\text{ex})}$  is obtained by replacing  $\mathbf{k}_f, s_f$  with  $\boldsymbol{\kappa}_f, \sigma_f$  in the direct term (2.1). Formula (2.2) holds for unpolarized electrons and includes an average over initial and a sum over final spins.  $N_i$  is the occupation number of the initial subshell, but for states with total angular momentum  $j_i > \frac{1}{2}$ , an additional sum over the magnetic quantum number  $|m_i|$  must be accounted for instead [16].

## III. LIGHT SYSTEMS

In the nonrelativistic case, the  $\boldsymbol{\alpha}_1 \boldsymbol{\alpha}_2$  coupling in the transition matrix element (2.1) can be disregarded, and the Darwin function turns into a bound-state Coulomb function. Since all electronic states are described by exact eigenstates to the same effective field, they are mutually orthogonal.

Whereas this is an advantage as compared to the plane-

wave Born approximation, the disadvantage of the Coulomb-Born theory is its neglect of proper screening. In the CBA, the effective charge of the wave functions is determined from the behavior of the initial-state function  $\phi_i$  near its shell radius  $a_i$  and will only lead to satisfactory results if ionization predominantly takes place in this spatial region. CBA results are therefore poor if the region far beyond the initial-state shell radius becomes important (for distant collisions), or in case of  $L$ -shell or higher-shell ionization, if close collisions select distances  $\ll a_i$ . In our calculations, Slater screening is used for the  $K$  shell, but for  $L$ -shell ionization of the light targets, we have made a more appropriate choice for  $Z_{\text{eff}}$ . Since the Fourier transform of  $\phi_i$  at small intrinsic momenta  $\boldsymbol{\kappa}_i$  governs the  $(e,2e)$  cross section in the binary peak region, which can readily be inferred from (2.1) by replacing the unbound electronic states with plane waves,  $Z_{\text{eff}}$  has been obtained by fitting the Fourier-transformed initial-state function resulting from an optimized potential calculation [17,18] at  $\boldsymbol{\kappa}_i = 0$  to the momentum-space Darwin function with charge  $Z_{\text{eff}}$ . This procedure leads to

$Z_{\text{eff}}=4.24$  for Ne and  $Z_{\text{eff}}=12.29$  for Ar.

The calculations to be presented below have been performed in coplanar geometry for scattering angles near the Bethe ridge. The Bethe ridge, which is characterized by a maximum yield of electrons, is defined through the momentum relation  $\mathbf{k}_i = \mathbf{k}_f + \boldsymbol{\kappa}_f$  such that the momentum transferred to the target nucleus is zero, or equivalently,  $\boldsymbol{\kappa}_i = \mathbf{0}$ . This leads to the condition for the scattering angle  $\vartheta_{k_f}$  of the projectile electron [16]

$$\cos \bar{\vartheta}_{k_f} = \frac{1}{2k_i k_f} (k_i^2 + k_f^2 - \kappa_f^2). \quad (3.1)$$

Figure 1 shows the  $2p$  subshell ionization of Ne by 8.2216-keV electrons at  $\vartheta_{k_f}=9.44^\circ$  (which is close to the Bethe ridge  $\vartheta_{k_f}=8.94^\circ$  for the energy sharing of 8 keV versus 200 eV). In the experimental data from Daoud and co-workers [9], the minimum at  $\vartheta_{k_f}=80.5^\circ$  from the angular structure of the  $p$ -state wave function is clearly seen. This minimum is considerably weaker in the CBA results. Moreover, CBA underestimates the peak intensity by  $\sim 50\%$ . This is due to the fact that the chosen  $Z_{\text{eff}}$  optimizes  $\phi_i$  and  $\phi_f$ , but underestimates screening for the projectile states in the binary region. This is readily seen from a comparison with the plane-wave CBA where complete screening is assumed for the projectile states ( $\psi_i$  and  $\psi_f$  being plane waves), which *overpredicts* experiment at the binary peak.

The situation is different in the recoil region, where both electrons are ejected into the same hemisphere (i.e., both azimuthal angles  $\varphi_{k_f} = \varphi_{\kappa_f} = 180^\circ$ , say). Here, close collisions are required, probing the wave functions near the origin. Our  $Z_{\text{eff}}$  is too small to account for sufficient reflection, such that CBA and also plane-wave CBA fall much below experiment.

When one moves away from the Bethe ridge to the region of small momentum transfer  $\mathbf{k}_i - \mathbf{k}_f$  to the projectile, the collisions become more distant such that the CBA becomes increasingly poorer for such light systems. If, for example, the scattering angle is decreased to  $\vartheta_{k_f} = 1.27^\circ$  while the other system parameters of Fig. 1 are unchanged, the experimental data [9] in the binary region are underestimated by the CBA by a factor of 15. Only plane-wave CBA results with a considerably lower charge for the ejected electron and an exact initial-state function  $\phi_i$  can reproduce the experimental binary peak intensity [9] (albeit not the recoil peak).

Figure 2 shows the situation for  $2p$  subshell ionization of the heavier Ar target at an impact energy of 3.249 keV, symmetric energy sharing and Bethe ridge conditions. Although the Ar  $L$  shell is an inner shell, the approximation of  $V(r)$  by an effective Coulomb field is not yet appropriate. In the binary peak region, the CBA falls below the DWBA by 50–80%, and the DWBA recoil peak around  $\vartheta_{k_f} = 20^\circ$  (for  $\varphi_{\kappa_f} = 180^\circ$ ) is not reproduced by the CBA. The experimental data of Hink and co-workers [19] are relative and are normalized to the DWBA calculations.

Unfortunately, no measurements or DWBA results are available for inner-shell ionization of heavier targets to bridge the gap between the Ar  $L$  shell where CBA is mostly poor and the Cu  $K$  shell where CBA is working [20]. By

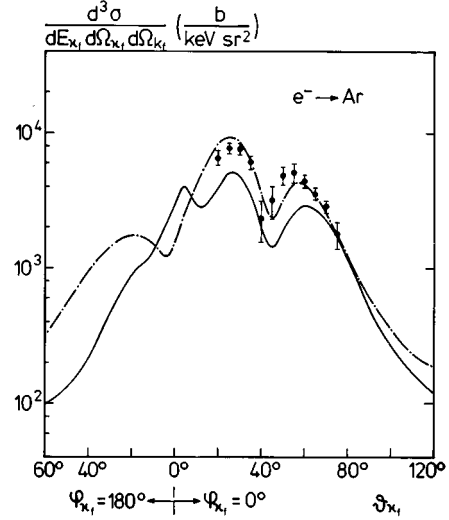


FIG. 2. Triply differential cross section for  $2p$  subshell ( $L_2 + L_3$ ) ionization of Ar by 3.249-keV electrons in coplanar geometry as a function of ejection angle  $\vartheta_{k_f}$ . The kinetic energies of the scattered and the ejected electron are equally 1.5 keV, the scattering angle  $\vartheta_{k_f} = 42.6^\circ$  is at the Bethe ridge, and the azimuthal angle is taken as  $\varphi_{k_f} = 180^\circ$ . Experiment: ●, Zhang *et al.* [19]. Theory: —, CBA with  $Z_{\text{eff}}=12.29$ ; - - - -, DWBA [19]. The experimental data are normalized to the DWBA.

testing the CBA for Ne and Ar at different collision energies, energy sharing, and scattering angles we have come to the following conclusion. For light targets (or outer-shell ionization of heavier targets), CBA is in general not satisfactory, neither in the binary nor in the recoil region, but gives (in the binary region) better results the larger the Bethe ridge angle  $\bar{\vartheta}_{k_f}$ , i.e., at a given  $E_{k_i}$ , the more one approaches equal energy sharing of the two outgoing electrons [which may be shown with the help of (3.1)]. This fact can be related to the higher momentum transfer to the bound electron at larger  $\bar{\vartheta}_{k_f}$  which requires closer collisions between the projectile electron and the target. Then the field of a neutral atom as seen by the projectile is better reproduced by a screened Coulomb field.

For very light atoms such as He, the CBA was found to give quite good results for the binary peak in the case of coplanar symmetric geometry [13]. For helium, both nuclear charge and effective charge are rather small such that deviations between the exact wave functions and the model wave functions are not as serious as for Ne or Ar. Also for carbon  $K$ -shell ionization at very small scattering angles, the CBA seemingly gave a reasonable prescription of the data, in particular of the ratio between the recoil peak and the binary peak [21]. However, the comparison could not be made on an absolute scale, and hence should be treated with care: We have found that for  $K$ -shell ionization of the heavier Ne at a much larger scattering angle and much less asymmetric energy sharing [19], DWBA is in the binary region underestimated by our CBA results by a factor of 3, while the experimental peak shape is quite well reproduced. Also, the choice of  $Z_{\text{eff}}=10$  (i.e., the full target nuclear charge) for the collision parameters of Fig. 1 (except for changing  $\vartheta_{k_f}$  to

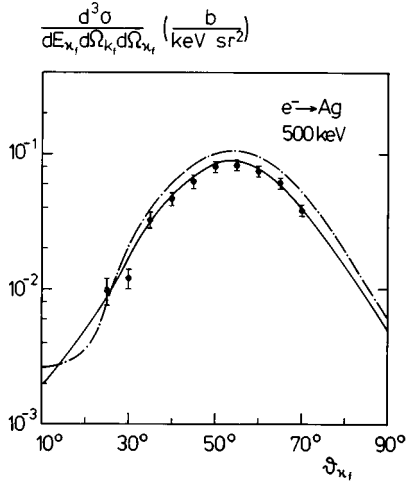


FIG. 3. Triply differential cross section for  $K$ -shell ionization of Ag by 500-keV electrons in coplanar geometry as a function of ejection angle  $\vartheta_{\kappa_f}$ . The parameters are  $E_{k_f} - mc^2 = 375$  keV,  $E_{k_r} - mc^2 = 99.5$  keV,  $\vartheta_{k_f} = 15^\circ$ ,  $\varphi_{k_f} = 180^\circ$  and  $\varphi_{k_r} = 0^\circ$ . Experiment:  $\bullet$ , Bonfert *et al.* [22]. Theory: —, CBA with  $Z_{\text{eff}} = Z - 0.3$ ; - - - -, DWBA [1].

1.27°) gives  $2p$  subshell CBA results that nicely describe both binary and recoil peak shapes, but that underpredict the experimental data [9] at all angles by one order of magnitude. Last but not least, even the slight underprediction of the symmetric Cu  $K$ -shell data by CBA at 500-keV impact energy [20] (as compared to 300-keV impact energy where  $\vartheta_{k_f}$  is larger) may be traced back to a too large  $Z_{\text{eff}}$  in the projectile scattering states.

#### IV. HEAVY SYSTEMS

The inner-shell ionization of heavy systems requires close collisions between the projectile electron and the target nucleus. In the case of  $K$ -shell ionization, particularly when both outgoing electrons are high in energy, screening effects by the passive electrons do not come into play. Also for  $L$ -shell ionization when  $Z - Z_{\text{eff}} \ll Z$  (with  $Z$  the target nuclear charge) screening will be of minor importance. Hence, there will be little difference in the results obtained from the CBA and the DWBA, provided that exact wave functions are used in the CBA. The comparison between our CBA and the DWBA therefore tests basically the quality of the semirelativistic wave functions used in the present calculations. Since those wave functions are at most correct to the order of  $Z\alpha$ , the deviations between the DWBA and our CBA results are a direct measure of the importance of relativistic effects. From Fig. 3 it is evident that for  $K$ -shell ionization of Ag at 500-keV collision energy the CBA is in good agreement with the absolute experimental data of Bonfert, Graf, and Nakel [22] recorded in the binary region, and also with relativistic DWBA calculations [1]. Even for  $L_3$ -shell ionization of Au at 300-keV impact energy (in coplanar geometry with asymmetric energy sharing) the CBA theory [16] explains absolute experimental data [23] as well as do the DWBA calculations [24]. This demonstrates that screening and relativistic effects are indeed not very important for these cases.

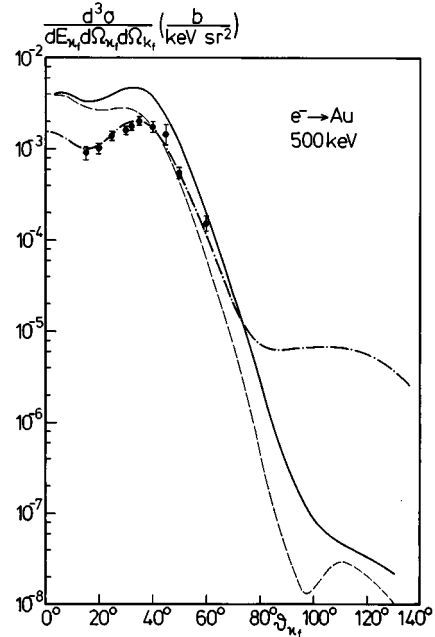


FIG. 4. Triply differential cross section for  $K$ -shell ionization of Au by 500-keV electrons in coplanar symmetric geometry ( $E_{k_f} = E_{k_r}$ ,  $\vartheta_{k_f} = \vartheta_{k_r}$ ,  $\varphi_{k_f} = 180^\circ$ ,  $\varphi_{k_r} = 0^\circ$ ) as a function of ejection angle  $\vartheta_{\kappa_f}$ . Experiment:  $\bullet$ , Bonfert *et al.* [22]. Theory: CBA with (—) and without (---) spin-flip contributions; - · - · -, DWBA [3].

In Fig. 4  $K$ -shell ionization of Au by 500-keV electrons is considered in coplanar symmetric geometry. Since the Au  $K$  shell is strongly relativistic, our CBA is inferior to the DWBA. Indeed, CBA overestimates the experimental data [22] and the DWBA results [3] by a factor 2–3 in the binary region and decreases dramatically towards the large-angle region where the DWBA predicts a second peak. This CBA deficiency is caused by the semirelativistic Darwin functions not being singular at the origin like the exact wave functions or the relativistic Coulomb waves. The missing spatial contraction is particularly serious in very close collisions (i.e., at large angles in the binary region or in the recoil region), resulting in much too small cross sections. The existence of a large-angle peak near  $110^\circ$  in the CBA contribution that excludes spin flip during the collision points to the fact that the missing spatial contraction affects mostly the spin-flip terms, the presence of which is a purely relativistic effect.

As another comparison between CBA and DWBA we have chosen a geometry that has recently been put forth by Whelan *et al.* [25], called “coplanar constant  $\Theta_{12}$  geometry.” In this geometry,  $\mathbf{k}_i$ ,  $\mathbf{k}_f$ , and  $\mathbf{\kappa}_f$  are in plane, and the angle  $\Theta_{12}$  between the momenta  $\mathbf{k}_f$  and  $\mathbf{\kappa}_f$  of the two outgoing electrons is kept constant while  $\mathbf{k}_f$  and  $\mathbf{\kappa}_f$  rotate around an axis perpendicular to the scattering plane. In Fig. 5 the  $K$ -shell ionization of Ag and Au by 300-keV electrons is shown for  $\Theta_{12} = 60^\circ$  and equal energy sharing. When  $\vartheta_{\kappa_f} = 30^\circ$ , one electron is ejected into the left hemisphere ( $\vartheta_{k_f} = 30^\circ$ ,  $\varphi_{k_f} = 180^\circ$ ) while the other one is found (symmetrically to the beam direction) in the right hemisphere ( $\vartheta_{\kappa_f} = 30^\circ$ ,  $\varphi_{\kappa_f} = 0^\circ$ ). Due to exchange symmetry, the angular distribution is symmetric with respect to  $\vartheta_{\kappa_f} = \Theta_{12}/2$  and

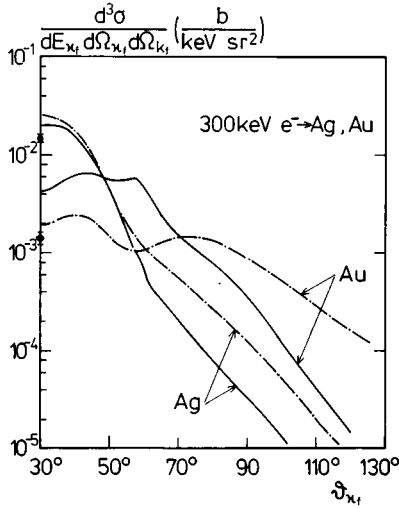


FIG. 5. Triply differential cross section for  $K$ -shell ionization of Ag and Au by 300-keV electrons in coplanar constant  $\Theta_{12}$  geometry ( $E_{k_f} = E_{\kappa_f}$ ,  $\vartheta_{k_f} = |\vartheta_{\kappa_f} - \theta_{12}|$ ) with  $\theta_{12} = 60^\circ$  as a function of ejection angle  $\vartheta_{\kappa_f}$ . The azimuthal angles are  $\varphi_{k_f} = 0^\circ$  and  $\varphi_{k_f} = 180^\circ$  for  $\vartheta_{\kappa_f} \leq 60^\circ$ , but  $\varphi_{k_f} = 0^\circ$  for  $\vartheta_{\kappa_f} > 60^\circ$ . —, CBA; - - - -, DWBA [25]. The two data points at  $30^\circ$  are from Bonfert *et al.* [22],  $\bullet$ , Ag;  $\blacklozenge$ , Au.

therefore only shown for  $\vartheta_{\kappa_f} \geq 30^\circ$ . When  $\vartheta_{\kappa_f}$  is increased beyond  $60^\circ$ , one passes from the binary region ( $\vartheta_{\kappa_f} < \Theta_{12}$ ) to the recoil region ( $\vartheta_{\kappa_f} > \Theta_{12}$ ) where  $\varphi_{k_f} = \varphi_{\kappa_f} = 0$ . For Ag, CBA is fairly close to the DWBA for  $\vartheta_{\kappa_f} \leq 60^\circ$  and falls below DWBA by a factor of 2–3 for the larger angles while showing approximately the same slope. For Au, however, CBA strongly overestimates DWBA in the binary region and drops much below DWBA for  $\vartheta_{\kappa_f} > 70^\circ$ . Also, the recoil peak of the DWBA at  $80^\circ$  is absent in the CBA where instead a second maximum appears in the binary-recoil transition region near  $60^\circ$ .

Most ( $e, 2e$ ) work has concentrated on the angular variation of the triply differential cross section for fixed energy sharing of the two outgoing electrons. However, in an early paper [27] on relativistic ( $e, 2e$ ) processes the dependence of the cross section on the energy of the ejected electron for fixed emission and scattering directions was also studied. Increasing the energy of the slower electron means selecting closer and closer collisions in a similar way as is achieved when at fixed energy, the emission angle is increased beyond the binary peak. In Fig. 6 we show such an energy dependence for 500-keV electron impact ionization of Ag. No DWBA spectra are available, so we can only compare CBA with the  $K$ -shell data from Schüle and Nakel [27]. These data are some 50% above theory at the higher energies, but a remeasurement with an improved apparatus [28] at 375 keV gives a lower electron yield in better agreement with CBA. Included in the figure are predictions for  $L$ -subshell ionization. According to the narrower momentum distribution of the  $L$ -shell electrons, the increase of the differential cross section with  $E_{\kappa_f}$  is stronger than for the  $K$  shell, such that  $L$ -shell ionization dominates when the Bethe ridge is approached. The same effect is seen for the  $2p$  subshell as compared to the more tightly bound  $2s$  subshell.

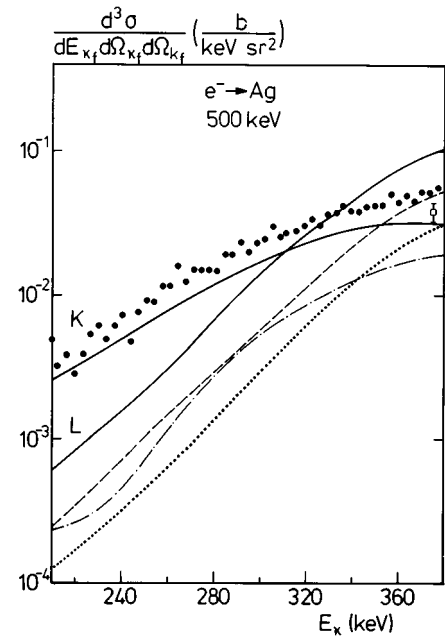


FIG. 6. Triply differential cross section for  $K$ - and  $L$ -subshell ionization of Ag by 500-keV electrons in coplanar geometry as a function of kinetic ejection energy  $E_{\kappa} = E_{\kappa_f} - mc^2$ . The angles are  $\vartheta_{k_f} = 40^\circ$ ,  $\vartheta_{\kappa_f} = 20^\circ$ ,  $\varphi_{k_f} = 180^\circ$ , and  $\varphi_{\kappa_f} = 0^\circ$ . Experiment for  $K$ -shell ionization:  $\bullet$ , Schüle and Nakel [27],  $\square$ , Nakel [28]. CBA theory (with Slater-screened  $Z_{\text{eff}}$ ): —,  $K$ -shell and total  $L$ -shell ionization (marked with  $K$  and  $L$ , respectively); - - - -,  $L_1$  shell;  $\cdots \cdots$ ,  $L_2$  shell; - · - · - ·,  $L_3$ -shell ionization.

At the Bethe ridge where the electron intensities have their largest values, the cross sections are particularly sensitive to structures in the wave functions. In order to obtain the Bethe ridge conditions for the spectra, one can use the energy conservation (2.3) and eliminate  $\kappa_f^2$  by means of the Bethe ridge formula (3.1), such that for a given  $\vartheta_{k_f}$  the two energies  $E_{k_f}$  and  $E_{\kappa_f}$  are determined. However, the second angle  $\vartheta_{\kappa_f}$  must be chosen to satisfy the momentum relation  $\mathbf{k}_f = \mathbf{k}_i - \mathbf{\kappa}_f$ .

Figure 7 shows the energy variation of the ejected Ag  $2p_{3/2}$  electrons across the Bethe ridge. For the scattering angle  $\vartheta_{k_f} = 51.2^\circ$ , one finds  $\bar{E}_{k_f} - mc^2 = 146.65$  keV and  $\bar{E}_{\kappa_f} - mc^2 = 350$  keV, as well as  $\bar{\vartheta}_{\kappa_f} = 27.8^\circ$ . Whereas  $s$  electrons show a simple maximum, the  $2p$  states have a dip in their energy dependence. Such a dip is known from the angular dependence of  $2p$  ionization across the Bethe ridge [6,16,19], and is related to the structure of the bound-state wave function in momentum space. When the Bethe ridge conditions are slightly detuned by changing the ejection angle, the  $2p$  minimum rapidly disappears, and the region of maximum intensity is shifted to different values of  $E_{\kappa_f}$ . This energy shift is much more pronounced than the shift of the peak intensity in angle when the angular dependence of the Bethe ridge detuning is studied [16].

Until now, we have exclusively considered the emission of the target electron in the scattering plane (the so-called coplanar geometry). In Fig. 8 we show predictions for non-coplanar emission for the case of Ag  $K$ -shell ionization by

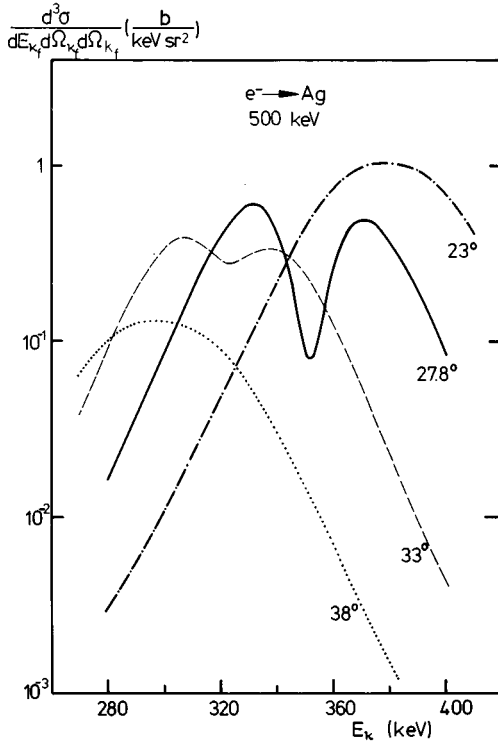


FIG. 7. Triply differential cross section for  $L_3$ -shell ionization of Ag by 500-keV electrons in coplanar geometry as a function of kinetic ejection energy  $E_k = E_{k_f} - mc^2$  at different ejection angles  $\vartheta_{k_f}$ . The other angles are fixed at  $\vartheta_{k_i} = 51.2^\circ$ ,  $\varphi_{k_f} = 180^\circ$ , and  $\varphi_{k_i} = 0^\circ$ . CBA theory:  $\cdots\cdots$ ,  $\vartheta_{k_f} = 23^\circ$ ;  $---$ ,  $27.8^\circ$ ;  $-\cdot-\cdot-\cdot$ ,  $33^\circ$ ; and  $\cdots\cdots$ ,  $38^\circ$ .

300-keV electrons. The  $(e, 2e)$  cross section is plotted for various tilt angles  $\psi$  of the beam direction  $\hat{\mathbf{k}}_i$  with respect to the plane spanned by the two outgoing electrons. Such a geometry has been considered by Murray and Read [29] in the context of helium ionization. The coplanar case is specified by  $\psi = 0$ , the scattering angle  $\vartheta_{k_f}$  is taken to be  $26.07^\circ$ , and the emission angle  $\vartheta_{k_i}$  is varied. In this case, the CBA compares well with the experimental data from Schröter *et al.* [30]. For  $\psi \neq 0$ , the direction of the scattering electron is kept fixed, but the angles are renamed from  $\vartheta_{k_f}$ ,  $\vartheta_{k_i}$  to  $\xi_{k_f}$ ,  $\xi_{k_i}$  since they are no longer the polar angles with respect to  $\hat{\mathbf{k}}_i$ .

From Fig. 8 it follows that the electron intensity strongly decreases with  $\psi$  while the peak gets broader, indicating that a large momentum has to be transferred to the target nucleus to allow for an out-of-plane ejection of the electron. Likewise, we have found that the  $2p$  dip that exists for the coplanar case at the Bethe ridge is rapidly damped out when  $\hat{\mathbf{k}}_i$  is tilted while, again, the intensity drops by several orders of magnitude upon increasing  $\psi$  from  $0^\circ$  to  $45^\circ$ . This has to be contrasted with earlier results on helium impact ionization by rather slow electrons where at  $\psi = 45^\circ$  the peak intensity has decreased by less than one order of magnitude [29] as compared to  $\psi = 0$ . Hence, it will be quite difficult experimentally to detect out-of-plane electrons at relativistic velocities.

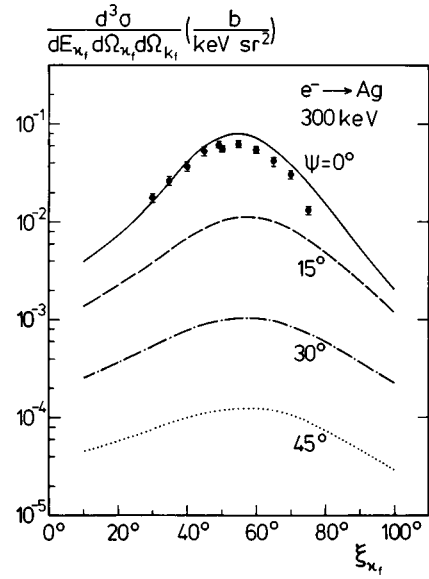


FIG. 8. Triply differential cross section for  $K$ -shell ionization of Ag by 300-keV electrons as a function of the angle  $\xi_{k_i}$  at different tilt angles  $\psi$  of the beam direction with respect to the scattering plane. The kinetic energies of the outgoing electrons are  $E_{k_f} - mc^2 = 200$  keV and  $E_{k_i} - mc^2 = 74.5$  keV. Experiment for coplanar geometry ( $\psi = 0$ ) at  $\vartheta_{k_f} = 26.07^\circ$ :  $\bullet$ , Schröter *et al.* [30]. CBA calculations (at  $\xi_{k_f} = 26.07^\circ$ ):  $---$ ,  $\psi = 0^\circ$ ;  $----$ ,  $15^\circ$ ;  $-\cdot-\cdot-\cdot$ ,  $30^\circ$ ; and  $\cdots\cdots$ ,  $45^\circ$ .

## V. ORTHOGONALIZATION OF THE SEMIRELATIVISTIC CBA

It was argued from plane-wave CBA results that the large differences occurring in the binary and recoil region when exact relativistic eigenstates were used on one hand and semirelativistic Coulomb functions on the other hand would to a large extent be due to nonorthogonality of the latter wave functions [8]. Indeed, when ionization is treated in the framework of a one-electron process induced by a perturber field, orthogonality between the initially bound electronic state and the continuum final state is required in order to avoid spurious overlap terms. The wave functions used in the semirelativistic CBA also do not meet this requirement. However, since the bound-state Darwin functions are constructed from the nonrelativistic Coulomb functions, the overlap terms result only from the relativistic corrections. In order to clarify the importance of such overlap terms, the CBA is modified by replacing the continuum state  $\phi_f^{(\sigma_f)}$  by a state  $\varphi_{\kappa_f}^{(\sigma_f)}$ , which is orthogonalized to the Darwin function  $\phi_i^{(\sigma_i)}$  by means of

$$\varphi_{\kappa_f}^{(\sigma_f)}(\mathbf{r}) = \phi_f^{(\sigma_f)}(\mathbf{r}) - \langle \phi_i^{(\sigma_i)} | \phi_f^{(\sigma_f)} \rangle \phi_i^{(\sigma_i)}(\mathbf{r}). \quad (5.1)$$

Due to the short range of the bound-state wave function, this orthogonalization procedure changes  $\phi_f^{(\sigma_f)}$  only at small distances and so does not affect its normalization, which is completely specified by the large- $r$  behavior. With (5.1), the transition matrix element now reads

$$W_{s_f\sigma_f s_i\sigma_i}^{d,\text{ortho}}(\mathbf{k}_f, \boldsymbol{\kappa}_f) = W_{s_f\sigma_f s_i\sigma_i}^d(\mathbf{k}_f, \boldsymbol{\kappa}_f) - \int \frac{d\mathbf{q}}{q^2 - q_0^2 - i\epsilon} \langle \phi_f^{(\sigma_f)}(\mathbf{r}_2) | \phi_i^{(\sigma_i)}(\mathbf{r}_2) \rangle \langle \psi_f^{(s_f)}(\mathbf{r}_1) \phi_i^{(\sigma_i)}(\mathbf{r}_2) | e^{i\mathbf{q}\cdot(\mathbf{r}_2 - \mathbf{r}_1)} (1 - \boldsymbol{\alpha}_1 \boldsymbol{\alpha}_2) \times | \psi_i^{(s_i)}(\mathbf{r}_1) \phi_i^{(\sigma_i)}(\mathbf{r}_2) \rangle, \quad (5.2)$$

with  $W_{s_f\sigma_f s_i\sigma_i}^d(\mathbf{k}_f, \boldsymbol{\kappa}_f)$  from (2.1). The exchange term  $W_{s_f\sigma_f s_i\sigma_i}^{\text{ex,ortho}}(\mathbf{k}_f, \boldsymbol{\kappa}_f)$  is, as in the conventional version of the CBA, obtained from (5.2) by interchanging  $\mathbf{k}_f, s_f$  with  $\boldsymbol{\kappa}_f, \sigma_f$  such that orthogonality is also preserved in the exchange term. However, one should keep in mind that this is an approximate consideration of exchange, and not exact, like in the nonorthogonalized CBA.

We have tested the effect of orthogonalization by calculating triply differential cross sections for  $K$ -shell ionization from (2.2) with the matrix element (5.2) and comparing it with our conventional CBA where the matrix element (2.1) is used. As a first example, we have studied the ionization of Ag by 300-keV electrons in asymmetric coplanar geometry ( $\vartheta_{k_f} = 10^\circ$ ,  $E_{k_f} - mc^2 = 200$  keV,  $E_{\kappa_f} - mc^2 = 74.5$  keV) where the conventional CBA reproduces the experimental data [26] in the binary peak but underpredicts experiment in the large-angle and recoil regions [16]. We have found a slight reduction by 2–3% in the binary region when the orthogonalized CBA is used, whereas in the large-angle and recoil regions the cross section is increased by at most 10%. Figure 9 shows a similar case,  $K$ -shell ionization of Ag by 500-keV electrons. Again it is obvious that the orthogonalization affects the electron intensity basically in the large-angle and recoil regions, but that it can by no means explain the large recoil peak that is found in experiment [22] or in the DWBA calculation [1].

In another example, ionization of Cu, Ag, and Au by 300- and 500-keV electrons in coplanar symmetric geometry [11,20], the effect is even less: Consideration of orthogonality lowers the cross section in the binary region by 1–2% for 500-keV Au, but much below 1% for the lighter targets. Since our approximate method for considering orthogonality shows that its effect is small in the semirelativistic CBA, we conjecture that this will also be true for a rigorous treatment of the orthogonalization procedure. Such a treatment would involve the Schmidt orthogonalization, which assures that all final states (not only the one with momentum  $\boldsymbol{\kappa}_f$ ) are orthogonal to  $\phi_i^{(\sigma_i)}$  while remaining mutually orthonormalized. One should, however, keep in mind that electron impact ionization of neutral atoms is actually a multielectron process, rather than a one-electron process, such that orthogonality between all initial and final states is not implemented from the outset (strictly speaking, the incoming electron feels a short-range field while each outgoing electron experiences an ionic field partly screened by the presence of the other electron).

## VI. CONCLUSION

The Coulomb-Born approximation has been applied to the calculation of  $(e, 2e)$  cross sections for a large variety of target atoms. Both angular and energy distributions of the

outgoing electrons were studied. For the  $L_3$  electrons at Bethe ridge conditions, a dip was not only found in the angular dependence but also in the spectra of the electrons. Moreover, when the coplanar geometry was abandoned by tilting the beam axis out of the detection plane, the intensity of the emitted electrons decreased rapidly, much more than for very light targets.

By comparing the CBA results with the more sophisticated DWBA and with experimental data we were able to test the validity of our theory. For light targets such as Ne or Ar, the difference between CBA and DWBA is the very crude account of screening by the passive electrons in the former theory. It was shown that this clearly is not sufficient and leads to a serious underprediction of the electron intensity in the binary peak area, more so the smaller the scattering angle and the energy of the ejected electron. Such screening effects are also expected to hamper the accuracy of the CBA results for outer-shell ionization of the heavier targets.

For the innermost shells of heavy targets screening is no longer of any consequence, but relativistic effects come into play. In this respect, the semirelativistic CBA theory used in this work has two shortcomings. One is the nonorthogonality of the Darwin bound state and the continuum functions. We could show by means of an approximate orthogonalization procedure that in the cases investigated the cross sections hardly changed, such that nonorthogonality in the CBA can be excluded as a possible source of error.

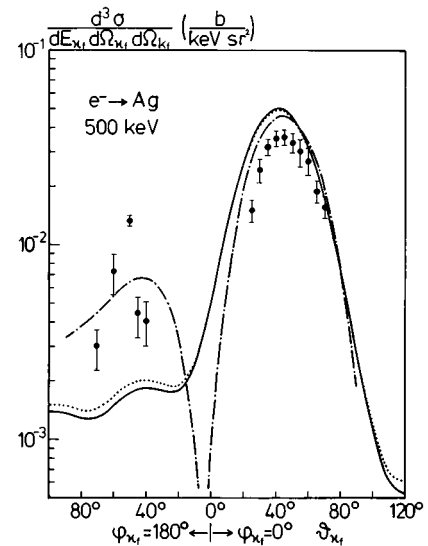


FIG. 9. Triply differential cross section for  $K$ -shell ionization of Ag by 500-keV electrons as a function of ejection angle  $\vartheta_{\kappa_f}$ . The scattering angle is  $7^\circ$ , the kinetic energy of the ejected and scattered electron is 99.5 and 375 keV, respectively, and  $\varphi_{k_f} = 0^\circ$ . Experiment:  $\bullet$ , Bonfert *et al.* [22]. Theory: —, CBA;  $\cdots$ , orthogonalized CBA;  $-\cdot-\cdot-\cdot-$ , DWBA [1].

The second shortcoming is the missing relativistic spatial contraction in the Darwin functions, which are only accurate to first order in  $Z\alpha$ . Comparing the present results with the relativistic DWBA theory we are led to the following conclusion. For weakly relativistic systems (such as the  $K$  shell of Ag or the  $L$  shell of Au) the semirelativistic CBA works excellently in the binary peak area. This is, however, no longer true for strongly relativistic systems (e.g., the  $K$  shell of Au). Also in the large-angle or recoil region where for the heavy targets very close collisions are required, the present theory strongly underestimates the intensity of the emitted

electrons. Improved results will only be obtained by using CBA with exact relativistic Coulomb waves.

#### ACKNOWLEDGMENTS

I would like to thank P. A. Amundsen for helpful comments and for calculating accurate bound-state Fourier transforms. I would also like to thank S. Keller and W. Nakel for discussions and for the communication of unpublished results. Support from GSI Darmstadt is gratefully acknowledged.

- 
- [1] S. Keller, C. T. Whelan, H. Ast, H. R. J. Walters, and R. M. Dreizler, *Phys. Rev. A* **50**, 3865 (1994).
  - [2] X. Zhang, C. T. Whelan, and H. R. J. Walters, *J. Phys. B* **23**, L509 (1990).
  - [3] C. T. Whelan, H. Ast, S. Keller, H. R. J. Walters, and R. M. Dreizler, *J. Phys. B* **28**, L33 (1995).
  - [4] D. H. Madison, I. E. McCarthy, and X. Zhang, *J. Phys. B* **22**, 2041 (1989).
  - [5] C. Dal Cappello, C. Tavad, A. Lahmam-Bennani, and M. C. Dal Cappello, *J. Phys. B* **17**, 4557 (1984).
  - [6] S. Keller and C. T. Whelan, *J. Phys. B* **27**, L771 (1994).
  - [7] A. Daoud, A. Lahmam-Bennani, A. Duguet, C. Dal Cappello, and C. Tavad, *J. Phys. B* **18**, 141 (1985).
  - [8] S. Keller, R. M. Dreizler, L. U. Ancarani, H. R. J. Walters, H. Ast, and C. T. Whelan, *Z. Phys. D* (to be published).
  - [9] A. Lahman-Bennani, H. F. Wellenstein, A. Duguet, and A. Daoud, *Phys. Rev. A* **30**, 1511 (1984).
  - [10] A. Lahmam-Bennani, *J. Phys. B* **24**, 2401 (1991).
  - [11] H. R. J. Walters, H. Ast, C. T. Whelan, R. M. Dreizler, H. Graf, C. D. Schröter, J. Bonfert, and W. Nakel, *Z. Phys. D* **23**, 353 (1992).
  - [12] D. H. Jakubassa-Amundsen, *Z. Phys. D* **11**, 305 (1989).
  - [13] J. Botero and J. H. Macek, *J. Phys. B* **24**, L405 (1991).
  - [14] C. Möller, *Ann. Phys. (Leipzig)* **14**, 531 (1932).
  - [15] B. L. Moiseiwitsch, *Adv. At. Mol. Phys.* **16**, 281 (1980).
  - [16] D. H. Jakubassa-Amundsen, *J. Phys. B* **28**, 259 (1995).
  - [17] K. Aashamar and P. A. Amundsen, *J. Phys. B* **21**, 2709 (1988).
  - [18] P. A. Amundsen (private communication).
  - [19] X. Zhang, C. T. Whelan, H. R. J. Walters, R. J. Allan, P. Bickert, W. Hink, and S. Schönberger, *J. Phys. B* **25**, 4325 (1992).
  - [20] D. H. Jakubassa-Amundsen, *J. Phys. B* **25**, 1297 (1992).
  - [21] J. Botero and J. H. Macek, *Phys. Rev. A* **45**, 154 (1992).
  - [22] J. Bonfert, H. Graf, and W. Nakel, *J. Phys. B* **24**, 1423 (1991).
  - [23] W. Nakel (private communication).
  - [24] S. Keller (private communication).
  - [25] C. T. Whelan, H. Ast, H. R. J. Walters, S. Keller, and R. M. Dreizler, *Phys. Rev. A* (to be published).
  - [26] H.-Th. Prinz, K.-H. Besch, and W. Nakel, *Phys. Rev. Lett.* **74**, 243 (1995).
  - [27] E. Schüle and W. Nakel, *J. Phys. B* **15**, L639 (1982).
  - [28] H. Graf, thesis, University of Tübingen, 1991.
  - [29] A. J. Murray and F. H. Read, *Phys. Rev. A* **47**, 3724 (1993).
  - [30] C. D. Schröter, H.-Th. Prinz, N. Keuler, and W. Nakel, *(e,2e) and Related Processes*, Vol. 414 of *NATO Advanced Study Institute, Series C*, Vol. 414, edited by C. T. Whelan *et al.* (Kluwer, Dordrecht, 1993), p. 403.